

# **IMMOBILISATION OF METAL ORGANIC FRAMEWORKS IN ELECTROSPUN POLYSTYRENE NANOFIBERS**

A THESIS SUBMITTED IN PARTIAL FULFILLMENT OF THE  
REQUIREMENT FOR THE AWARD OF THE DEGREE OF

**MASTER OF TECHNOLOGY**  
(POLYMER TECHNOLOGY)  
TO

**DELHI TECHNOLOGICAL UNIVERSITY**



SUBMITTED BY  
**HARSHIT VARSHNEY**  
ROLL NO:- 2K14/PTE /04

UNDER THE GUIDANCE OF  
**Dr. PRASUN K ROY**  
SCIENTIST 'E'

**CENTRE FOR FIRE EXPLOSIVE AND ENVIRONMENT SAFETY (CFEES)**  
**DEFENSE RESEARCH & DEVELOPMENT ORGANISATION (DRDO)**  
**TIMARPUR, DELHI 110054**

&  
**Dr. D. Kumar**  
**PROFESSOR**  
**DEPARTMENT OF APPLIED CHEMISTRY**  
**AND POLYMER TECHNOLOGY**  
**DELHI TECHNOLOGICAL UNIVERSITY**  
(FORMERLY DELHI COLLEGE OF ENGINEERING)  
**BAWANA ROAD, DELHI-110042**  
**JUNE 2016**

## CERTIFICATE

---

This is to certify that the M.Tech major project thesis entitled “**Immobilisation of Metal Organic Frameworks in electrospun polystyrene nanofibers**” has been submitted by HARSHIT VARSHNEY, for the award of the degree of “Master of Technology” in Polymer Technology is a record of bonafide work carried out by him. Harshit has worked under our guidance and supervision and fulfilled the requirements for the submission of the thesis. The project work has been carried out during the session 2015-2016.

To the best of our knowledge and belief the content therein is his original work and has not been submitted to any other university or institute for the award of any degree or diploma.

**Dr. D. KUMAR**  
**PROFESSOR**  
DEPARTMENT OF APPLIED  
CHEMISTRY AND POLYMER  
TECHNOLOGY  
DELHI TECHNOLOGICAL UNIVERSITY  
(*FORMERLY DELHI COLLEGE OF  
ENGINEERING*)  
DELHI-110042

**Dr. PRASUN K ROY**  
**SCIENTIST ‘E’**  
CENTRE FOR FIRE  
EXPLOSIVE AND  
ENVIRONMENT SAFETY  
(CFEES) DEFENSE  
RESEARCH AND  
DEVELOPMENT  
ORGANISATION (DRDO)  
TIMARPUR , DELHI 110054

## ACKNOWLEDGEMENT

---

I express my sincere thanks and deep sense of gratitude to my supervisors Dr. P.K. Roy (Scientist 'E', Centre for Fire, Explosive and Environment Safety (CFEES), DRDO) for his inspiring guidance, constant encouragement and motivation throughout the course of this work. To him I owe more than words can say, Dr. D. Kumar Professor for guiding me and helping me in all ways throughout my course work.

I take this opportunity to thank the management of CFEES, DRDO for giving me this opportunity to carry out this project work in their esteemed laboratory. It was a privilege to work under the esteemed guidance of Dr. Chitra Rajagopal (Group Head, 'ESG').

I would like to express my profound gratitude to Dr. R.C Sharma Head of Department, Department of Applied Chemistry D.T.U ,to all the faculty members and the non-teaching staff of Department of Applied Chemistry and Polymer Technology D.T.U. for helping me in all the related problems during the entire duration of , M.Tech.

I want to thank Mrs Manorma Tripathi, Mrs Surekha Parthasarathy, Mr. Rajesh Chopra, Mr. Naveen Saxena, Ms Pratibha Sharma, Mr. A.V Ullas, Mr. Nahid Iqbal for their immense support and guidance that helped me in completing the project.

I thank all the members of Centre for Fire Explosive and Environment Safety (CFEES) and DTU for their kind cooperation.

I thankfully acknowledge my family members and friends whose inspiration and motivation brought me to the completion of this project. This was a great learning experience and I will cherish it throughout my life.

DATE

(HARSHIT VARSHNEY)

# TABLE OF CONTENTS

LIST OF FIGURES .....	1
LIST OF TABLES.....	1
ABSTRACT.....	2
CHAPTER 1: INTRODUCTION AND LITERATURE SURVEY.....	3
1. Introduction .....	3
1.1 Metal organic frameworks .....	3
1.2 Polymer Nanofibers.....	6
1.2.1Electrospinning.....	7
1.2.2 Factors Affecting Properties of Electrospun Fibres .....	8
1.2.2.1Molecular weight, Viscosity and concentration .....	8
1.2.2.2 Solution conductivity.....	9
1.2.2.3Effect of voltage .....	9
1.2.2.4 Flow rate.....	9
1.2.2.5 Diameter of needle electrode .....	9
1.2.2.6 Distance between the Collector and the Tip of the Syringe .....	10
1.2.2.7 Mechanism of fiber formation in electrospinning .....	10
1.2.3 Applications of electrospun nanofibres.....	12
1.3 Ultrasonication .....	12
1.4 Aims and Objectives .....	13
CHAPTER 2: EXPERIMENTAL.....	14

2.1. Introduction .....	14
2.2. Materials .....	14
2.3. Electrospinning set up .....	14
2.3.1 Spinning unit .....	14
2.3.2 Control unit .....	15
2.3.3 Preparation of Polystyrene nanofibres .....	15
2.4 Preparation of Supramolecular assembly of Metal Organic frameworks[Zn <sub>4</sub> O(BDC) <sub>3</sub> , MOF-5].....	16
2.5 Ultrasonication .....	16
2.6 Preparation of MOF5 immobilised polystyrene nanofibres .....	17
<u>2.7. Characterization .....</u>	<u>19</u>
2.7.1 Structural characterization.....	19
2.7.1.1 Scanning Electron Microscopy.....	19
2.7.1.2 Powder X-rays Diffraction .....	20
2.7.2 FTIR .....	21
2.7.3 Thermal Characterization.....	22
2.7.3.1 Thermogravimetric Analysis .....	22
2.7.3.2. Differential Scanning Calorimetry .....	23
2.7.4 Surface area analysis .....	24
<b>CHAPTER 3: RESULTS AND DISCUSSION.....</b>	<b>26</b>
3.1 Supramolecular assembly of MOF-5. ....	26
3.2 Surface area analysis of MOF-5.....	26

3.3 Thermal analysis of MOF-5 .....	27
3.4 Electrospinning of polystyrene nanofibre .....	28
3.4.1 Effect of Concentration on the polystyrene fibre morphology .....	28
3.4.2 Effect of flow rate on polystyrene Nanofibre morphology .....	29
3.4.3 Thermal characterization of Polystyrene nanofibers .....	30
3.5. MOF-5 immobilised polystyrene fibers .....	31
3.5.1 Surface morphology of MOF-5 immobilised polystyrene fibers .....	31
3.5.2 Thermal analysis of MOF-5 immobilised polystyrene fibers .....	33
3.5.2.1 Thermo Gravimetric Analysis of MOF-5 immobilised polystyrene fibers .....	33
3.5.2.2 Differential Scanning Calorimetry of MOF-5 immobilised polystyrene fibers .....	34
3.5.4 Crystal structure of MOF-5 immobilised polystyrene fibers .....	35
3.5.5 FTIR of MOF-5 immobilised polystyrene fibers .....	36
CHAPTER 4: SUMMARY AND CONCLUSION .....	38
REFERENCES .....	40

## LIST OF FIGURES

<b>Figure1.1:</b> Structures of 1D, 2D, 3D coordination polymers.
<b>Figure1.2:</b> Schematic diagram of electrospinning process
<b>Figure1.3:</b> Schematic diagram illustration of the Taylor cone formation
<b>Figure1.4:</b> Schematic diagram showing applications of Nanofibers
<b>Figure1.5:</b> Schematic showing de-agglomeration due to ultrasonication
<b>Figure2.1:</b> Setup of an electrospinning unit
<b>Figure2.2:</b> i)Chemical structure of secondary building unit, ii) structure of Zn <sub>4</sub> O node and iii) 3 D structure of the framework of MOF-5
<b>Figure2.3 :</b> Ultrasonicator used for dispersion of MOF-5 in polystyrene solution
<b>Figure2.4 :</b> Scanning electron microscope
<b>Figure2.5 :</b> FTIR spectroscopy
<b>Figure2.6 :</b> TGA
<b>Figure2.7 :</b> DSC analyser
<b>Figure2.8 :</b> Surface area analyser
<b>Figure3.1 :</b> SEM micrograph of MOF-5
<b>Figure3.2 :</b> N <sub>2</sub> adsorption (open symbol) and desorption isotherms (closed symbol) for MOF-5.
<b>Figure3.3 :</b> TG-DTG traces of MOF5
<b>Figure3.4 :</b> Effect of concentration on the surface morphology of polystyrene nanofibers at different concentrations: <b>(a)</b> 5% (w/v) <b>(b)</b> 10 % ( w/v) <b>(c)</b> 15 % ( w/v) <b>(d)</b> 20 % ( w/v)
<b>Figure3.5 :</b> Effect of flow rate on the surface morphology of polystyrene nanofibers at different concentrations <b>(a)</b> 1 ml/h <b>(b)</b> 1.5 ml/h <b>(c)</b> 2ml/h
<b>Figure3.6 :</b> TG-DTG traces of Polystyrene fibers
<b>Figure3.7 :</b> SEM micrographs of MOF-5 immobilised polystyrene fibers at flow rate of 1.5 ml/h with MOF-5 concentration of a) 20% b) 100% c) 300% and d)500%
<b>Figure3.8 :</b> SEM micrograph of MOF-5 crystal on polystyrene fiber
<b>Figure3.9 :</b> TG traces of a) MOF2PS b)MOF8PS c)MOF20PS
<b>Figure3.10 :</b> DSC traces of MOF-5 loaded PS fibers
<b>Figure3.11 :</b> The PXRD of MOF-5 loaded PS fibers
<b>Figure3.12 :</b> FTIR spectra of a) PS4MOF b) MOF-5
<b>Figure3.13 :</b> FTIR spectra of a)TPA b) MOF-5

## LIST OF TABLES

Table 2.1 : Sample Designation
Table 3.1 : Thermal characteristics of decomposition

## ABSTRACT

The current technology of air-filtration materials for protection against highly toxic chemicals is primarily based on the broad and effective adsorptive properties of hydrophobic activated carbons. However, adsorption does not prevent these materials from behaving as secondary emitters once they are contaminated. Thus; the development of efficient self-cleaning filters is of high interest. The present work deals with the use of electrospinning technology to develop fibers incorporating metal organic framework molecules (MOFs) that exhibit the potential to selectively capture gases such as toxic industrial chemicals, providing a filtration system that can help protect first responders and others at high risk for exposure to such substances. MOFs are crystalline porous compounds that can be customized via nano-level manipulation to trap specific gases. In the present work, we have immobilised a highly celebrated metal organic framework i.e. MOF-5 in polystyrene (PS) fibers using the electrospinning technique. MOF-5 ( $Zn_4O(BDC)_3$ ) was chosen as an adsorbent in view of its exceptionally high surface area and its stability under the operating conditions employed during electrospinning. Nano-fibrous webs, being much lighter allows sufficient savings in terms of weight along with providing necessary strength and increased surface area can result in an exceptional increase in ability to attach or release, absorbed molecules, catalytic moieties, functional groups etc. thus can be used to make air filters or functional textiles.

[1]This thesis focuses on establishing the effect of increasing concentration of the polymer on the morphology of the electrospun fibers of polystyrene using Hamilton needle. The effect of increasing amounts of MOFs on electrospun fibers of polystyrene has also been studied in detail for potential application in the field of air filtration. Non-wovens mat were produced and characterized with regard to their stability, porosity and morphology.



# CHAPTER 1

## INTRODUCTION AND LITERATURE SURVEY

### 1. Introduction

It is of great interest to incorporate porous materials into polymeric Nanofibers with an aim to trap noxious gases and break them down into less harmful substances for decontamination.

A porous material is the one which has pores, more commonly referred as voids. The skeletal part of the material is often denoted as the "matrix" or "frame". The pores are distinctively filled with a fluid (liquid or gas). The most significant characteristic of a porous medium is its porosity. Frequently both the pore network and the solid matrix are continuous, in order to form interpenetrating continua such as in a sponge. Many natural substances such as soil, zeolites and rocks, and man-made materials such as ceramics are considered as porous media. By reckoning them to be porous media, many of their crucial properties can only be rationalised.

#### 1.1 Metal organic frameworks

Metal organic frameworks (MOFs) are a rising class of porous materials, which in perspective of their high surface area, uniform pore size, and thermal stability are potential candidates for several applications like filtration, storage, separation, sensing and catalysis[2], hence more than 20,000 different MOFs have been reported and studied. The accessibility of in-pore functionality and characteristic of outer-surface modification in MOFs made these materials highly interesting for various applications over porous aluminosilicates such as zeolites. Moreover, it is possible to vary the geometry and the pore size of the MOFs for the purpose of specific applications, which can be achieved by a prudent choice of the metal and linker units.

MOFs are currently at the vanguard of research as storage substrate for hydrogen and methane gas[3], carbon dioxide capture and storage[4, 5], and as a new and more efficient, selective, greener catalysts.[6, 7].The surface areas exhibited by these crystalline materials have exceeded that of many zeolites and activated carbon materials up to a great extent. There is a copious empirical literature which tells that there is a rampant possibility to create uniform pore sizes, selective uptake of small molecules, high apparent surface areas, and optical or magnetic responses on an inclusion of guest molecules[8]. Comparatively a new member to the family of porous solids, MOF research has expanded at a stupefying pace in the last decade [9].

Transition metal ions with multiple geometries and oxidation states are generally employed as the inorganic constituent of MOFs. Lanthanide ions have large coordination numbers (usually from 7 to 10) are also used to form new and unusual network topologies.

As far as the organic linker is concerned, an extensive variety of ligands are available. Ligands with rigid backbones prefer to be a choice, as the inherent rigidity gives a prediction of the network geometry. In addition, rigidity also provides strength to the open-pore structure after solvent removal, which remains entrapped during the synthesis. The linkers can be electrically neutral, cationic, or anionic. The most frequently used neutral organic linkers are pyrazine, imidazoles, and 4,4'-bipyridine (bpy). These linkers fulfill the purpose of pillars in the construction of pillared-layer in 3D networks. One of the anionic linkers that are most widely used is carboxylates, because of their capability to aggregate metal ions into clusters, thus forming a stable framework. Cationic organic ligands are rarely used, due to their low affinities towards cationic metal ions. Metal-Organic Frameworks are a subclass of coordination polymers, thus they are also coordination compounds with repeating coordination entities extending in one, two, or three dimensions[10].They can be considered as being constructed from two components. The figure1.1 below shows that by choosing

metal components ‘M’ and matching these with bridging ligand components that MOFs with different dimensionalities result. Most MOFs are formed in solution and crystallise from the reaction mixture. It might be perceived that the structures of 1D coordination polymers are simple, but when the 1D strands lay parallel or anti-parallel, crisscrossed, or be interwoven complex structures are often formed. In the case of 2D structure, nets can lie atop one another, similar to what is observed in the structure of natural clays, or they can also interpenetrate each other. The most interesting structure type is the 3D MOF polymer which is widely used for various applications. The blue sphere symbolizes the pore volume, which is the void inside the framework. In the case of 3D structure interpenetration of networks occurs and in all the cases, interpenetration leads to the reduction of the pore volume.

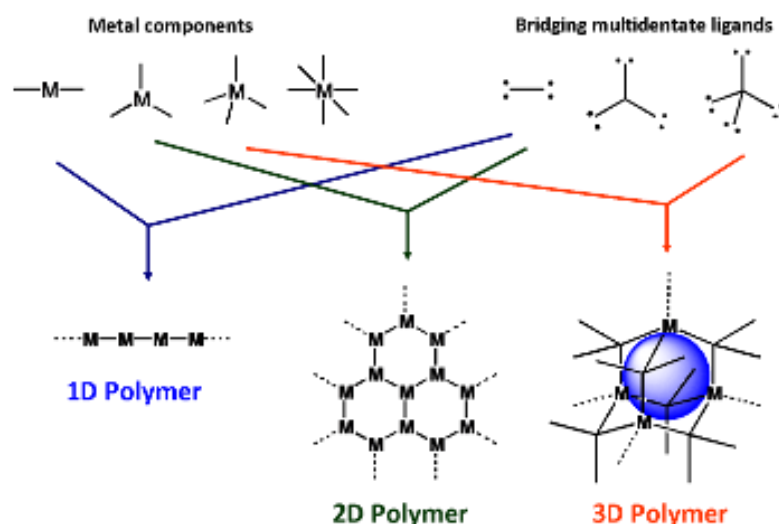


**Figure 1.1:** Structures of 1D, 2D, 3D coordination polymers.

MOFs are excellent materials for a variety of applications like gases storage such as carbon dioxide and hydrogen, purification of gases, gas separation, in catalysis and also as sensors, because of their salient features like ultra-high surface area, mend ability of pore structure, and a very high thermal and chemical stability. The permanent porosity is a key property for many of these applications. Early interest was to use their porous structure to store gases, particularly hydrogen gas for energy reasons. The availability of in-pore functionality and

modifiability of outer-surface in MOFs make them extremely charismatic in the context of gas or liquid separation. In this context, it is prudent to mention the use of zeolites, which have well-defined porous structures and diameter of pore closer to the dimension of small hydrocarbons. Zeolites are a type of aluminosilicates which have inorganic framework structures built by corner sharing of  $\text{SiO}_4$  and  $\text{AlO}_4$  tetrahedral; zeolites cause the separation of components on the basis of “molecular sieving”. The molecular sieving i.e. the ability to selectively sort molecules is a particular property of these materials, it is primarily based on a size exclusion process which is due to a very regular pore molecular structure dimensions. The chances of chemical interaction of the adsorbent with the zeolites are very distant in the absence of active sites. On the other hand is the secondary building unit of the MOF, that can be selected suitably from the transition metal series, which allows components to separate on the basis of molecular interaction of the stationary phase with the components.

## **1.2 Polymer Nanofibers**

Polymeric nanofibers production is a riveting area and is the focus of a great deal of research activity worldwide. The nano prefix is generally applied to materials with the dimensions less than 100nm, but in the case of fibers, the limit is up to 0.5  $\mu\text{m}$  or even 1 $\mu\text{m}$ . For simplicity, all sub-micron fiber can be considered as nanofibers. The preparation of polymeric nanofibers by electrospinning technique [11, 12] was first patented in 1902 and has gained increasing attention from last few decades. Nanofibers can also be prepared by several other techniques, e.g. drawing and template synthesis. ‘Drawing’ is similar to dry spinning, that is, it can make long single nanofibers; with the limitation that, it is applicable only for those viscoelastic materials that can undergo strong deformations while being cohesive enough to support the pulling stress. ‘Template synthesis’ is the one which uses nano-porous membrane as a template to make nanofibers. Unlike Drawing, it cannot make single continuous nanofibers. Relatively it is a time-consuming process. Among all these techniques,

‘Electrospinning’ is recognized as the most efficient technique, despite its limitations such as relatively low productivity. Mostly polymer solution and sometimes polymer melts are used in this technique to produce nanofibers. Most of these nanofibers were spun from solution, although spinning from the melt in vacuum and air are also possible. Melt electrospinning requires special heating assembly to keep the polymer in the molten form at the tip of the needle.

### **1.2.1 Electrospinning**

Electrospinning is a version of “Electro spraying’ process”. This technique has become important since 1994, though the fundamental idea of electrospinning is much older which dates back to 1934. Electrospinning is a very simple and versatile fiber forming process produced by pushing polymer solution (or polymer melt) mechanically through a nozzle under a high-voltage electric field. Formation of fibers in the electro spinning process is carried out by repulsive electrostatic forces. Electrostatic interactions in the charged fluid jet result in jet instabilities and elongation that cause the polymer jet to form a Taylor cone at the needle tip. The fluid jet leaving the tip undergoes stretching due to the intensive interaction of charged jet with the electric field. During this process, the solvent evaporates and charged nanofibers of few nanometres to few microns (usually between 50 and 900 nm) are formed. Mostly the nanofibers formed by this method are in the form of a random web and appear as a very fine spray or a film. Due to many research groups working in the field of tissue engineering scaffolds [13, 14], wound dressing materials [15], Nanocomposites, Nano sensors, etc. which demand highly skilled use of nanofibers, electrospinning has gained widespread popularity in recent times. Moreover, many research groups have spun nanofibers from different polymers such as nylon 6 [16] cellulose acetate, poly (vinyl alcohol) [17, 18], polyethylene terephthalate, polyacrylonitrile, polyurethanes, polystyrene [19], and many other polymers.

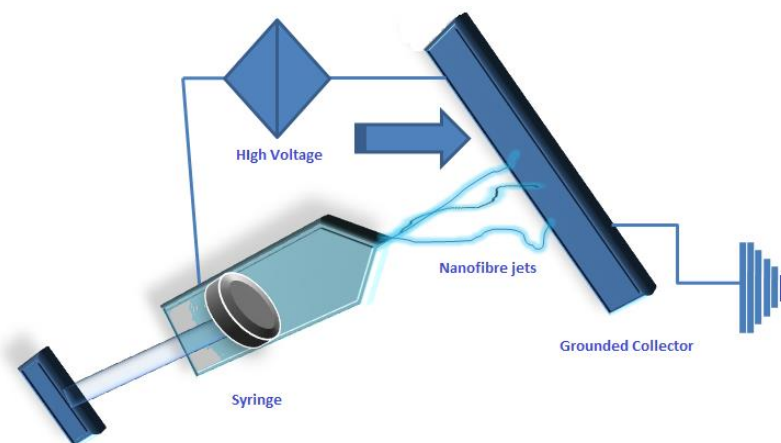


**Figure 1.2:** Schematic diagram of electrospinning process

## 1.2.2 Factors Affecting Properties of Electrospun Fibers

### 1.2.2.1 Molecular weight, Viscosity and concentration

The Molecular weight of polymer depends on the length of polymer chains and plays a vital role in deciding the morphology of electrospun fibre. Entanglements in the polymer chains decide whether the electrospinning jet breaks up into spray of small droplets or continuous fibers. At lower polymer concentration viscosity will be less thus fewer chain entanglements and the high amount of solvent molecules which means that surface tension has more influence over the fluid jet results in beads formation rather than smooth fibers. Higher the molecular weight better will be the entanglements in polymer chains in solution which results in a more viscous solution, thus smooth fiber will be obtained. In electrospinning process a minimum polymer concentration is required for the fiber formation to subsist. Below this critical value, the voltage applied leads to bead formation and electro spraying. With the increase in polymer concentration, an assortment of beads and fibers are formed. The spherical morphology gradually converts to spindle-like and eventually uniform fibers are formed due to the increment in concentration. The optimum concentration for electrospinning depends on the nature and molecular weight of the polymer. Entanglement density which

increases with the increase in concentration, molecular weight and also with the nature of solvent (better solvent higher entanglement density) decides the fiber formation. The high entanglement density leads to thicker fibers.

#### **1.2.2.2 Solution conductivity**

Electrospinning involves stretching of the fluid jet caused by electrostatic repulsion at its surface. If the solution has higher conductivity, more charges can be carried along by the fluid jet. The increased amount of charges will favor more stretching of the fluid jet which causes the formation of thinner fibers.

#### **1.2.2.3 Effect of voltage**

The fiber diameter decreases with the increment of the applied voltage. Higher voltage also has a greater probability of beads formation [21]. Thus, it can be said that voltage does influence fiber diameter, but the significant change in diameter also varies with the polymer solution concentration and the distance between the collector and the tip of the needle. [22]

#### **1.2.2.4 Flow rate.**

One of the important process parameters is the Flow rate. Flow rate defines the amount of solution available for electrospinning. Usually, a lower flow rate is preferred so that the polymer solution will get sufficient time for polarization. If the flow rate is very high, thick fibers with beads will form instead of the smooth thin fibers owing to the low stretching forces and less drying time ahead to reach the collector.

#### **1.2.2.5 Diameter of needle electrode**

Smaller the diameter of needle less will be the clogging of the polymer at the tip and smaller will be the diameter of the Electrospun fibers.

### 1.2.2.6 Distance between the Collector and the Tip of the Syringe

The fibers diameter and their morphology get affected by the distance between the tip of the needle and the collector. If the distance is less, there will not be enough time for the fibers to solidify prior to reaching the collector, vaporization of the solvent is very crucial for fiber formation, so optimum distance is recommended. It had been demonstrated that increasing the distance gives more time for the charged fluids to split and for the solvent to evaporate.[23]

### 1.2.2.7 Mechanism of fiber formation in electrospinning

The fiber formation mechanism in electrospinning is governed mainly by two factors, one is the amount of the electrostatic charges available on the surface of the fluid jet as a ramification of the generation of a very high potential difference, and other is the surface tension of the polymer solution, although there are other factors such as concentration of solution, viscosity, needle diameter, etc. which also play a vital role. The fiber forming process can be described by the following steps.

- The polymer solution is pushed through the syringe mechanically at the prescribed flow rate.
- The polymer droplet is held by its own surface tension at the tip of the needle electrode.
- The interaction of the polymer droplet with the external electric field force the droplet to assume a conical shape, known as **Taylor cone** due to simultaneous actions of repulsive forces of induced surface charge and the attractive forces of the surface tension of the solution.
- As the surface tension of the droplet is subdued, the droplet becomes unstable and a liquid jet is discharged.
- Electrostatic charges cause repulsion in the jet which leads to increase in surface area.



- The surface tension of the polymer solution causes reduction in the total surface of the jet, which leads to breaking up of jet into droplets, the process is called ‘electrospraying’
- Which of the two opposing effects dominate, will depend on the surface tension of the polymer solution and its viscosity.
- In this process, charged nanofibers are formed as the solvent evaporates. Generally, the nanofibers are obtained in the form of a random web which is made by this process and they appear like a very fine spray or a film.

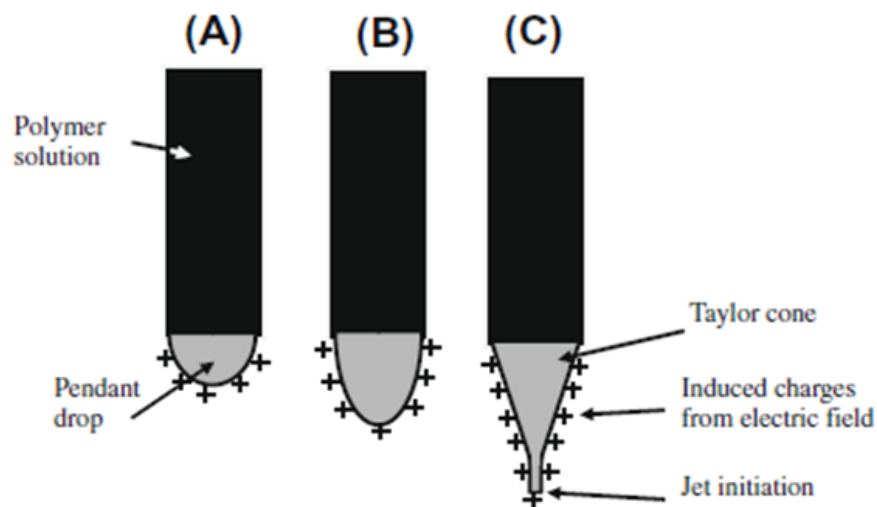


**Figure 1.3:** Schematic diagram illustration of the Taylor cone formation[20].

- (a) Surface charges are induced in the polymer solution due to the electric field.
- (b) Elongation of the pendant drop
- (c) Deformation of the pendant drop to the form the Taylor cone due to the charge repulsion and a fine jet initiate from the cone.

### 1.2.3 Applications of electrospun nanofibers

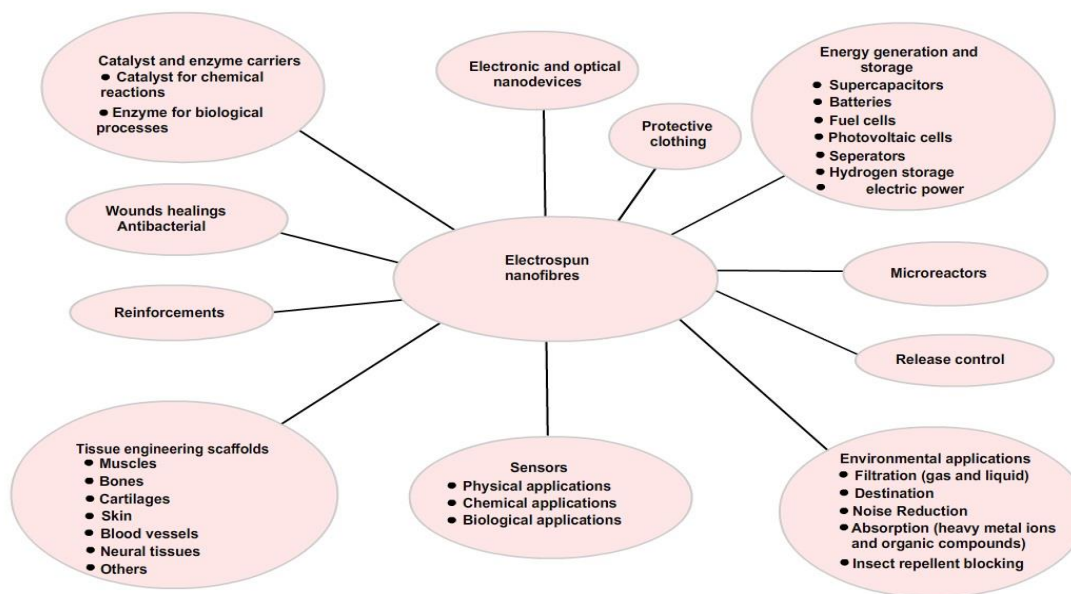


**Figure 1.4:** Schematic diagram showing applications of Nanofibers

### 1.3 Ultrasonication

Ultrasonication involves the irradiation of a liquid sample with ultrasonic waves of more than 20 kHz which results in agitation. Sound waves when to propagate into the liquid media cause an alternating high-pressure also called compression and low-pressure know as rarefaction cycles. During rarefaction, sonic waves of high-intensity generate small void or vacuum bubbles in the liquid, which then collapse aggressively i.e. cavitation during compression, stimulating very high local temperatures. Distribution and Dispersion of solids into liquids is a significant application of ultrasonic devices/processors. Ultrasonic cavitation generates shear forces of a very high magnitude that break the cluster of particles into single dispersed particles distributed uniformly in the liquid solution. The mixing of powders in a liquid solvent/solution is a usual step in the formulation of various products, like paints, inks, shampoos, beverages, or polishing media. The cluster of individual particles is formed due to various physical and chemical forces of attraction like van der Waals forces, liquid surface tension, etc. The attraction forces must be subdued in order to de-agglomerate and disperse

the particles in the liquid media. High-intensity ultrasonication is a better alternative to high-pressure homogenizers and rotor-stator-mixers for the dispersion and distribution of powders in liquids.

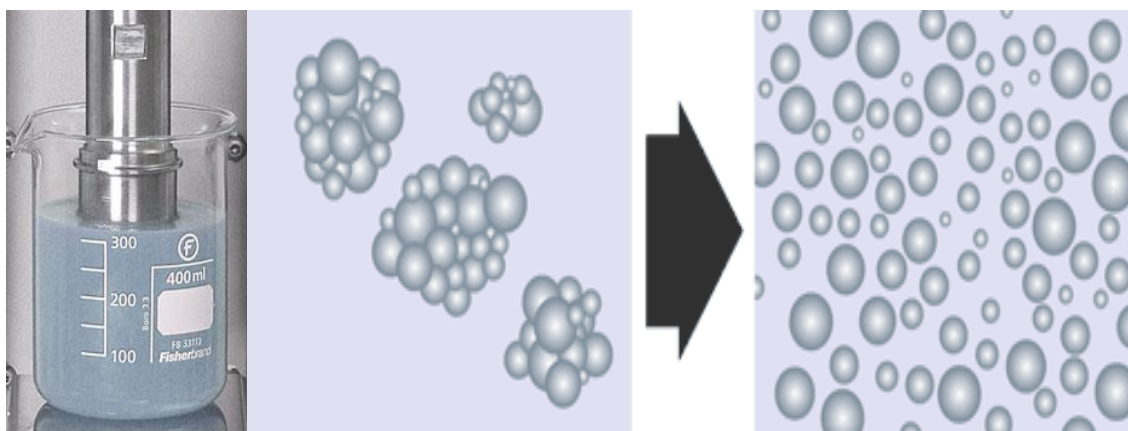


**Figure1.5 : Schematic showing de-agglomeration due to ultrasonication**

#### **1.4 Aims and Objectives**

This project deals with the electrospinning of polystyrene fibers containing high loadings of MOF-5 for potential application in the field of air filtration.

A systematic methodology highlighting the progress of the proposed work involves following steps:

- Preparation of MOF5
- Characterisation of MOF5
- Preparation of Polystyrene nanofibers by electrospinning
- Characterisation of Polystyrene nanofibers
- Dispersion and distribution of MOF-5 in the polymer solution by Ultrasonication.
- Preparation of MOF5 immobilised Polystyrene nanofibers by electrospinning.
- Characterisation of MOF5 immobilised Polystyrene nanofibers.

## CHAPTER 2

### EXPERIMENTAL

#### 2.1. Introduction

This section deals with the synthetic procedure involved in the preparation and characterisation of MOF-5, polystyrene nanofibers and MOF-5immobilised polystyrene nanofibers.

#### 2.2. Materials

Polystyrene (GPPS), zinc nitrate trihydrate ('AR' grade, E. Merck), terephthalic acid (TPA) ('AR' grade, E. Merck), N,N-dimethylformamide (DMF) ('AR' grade, E. Merck) and chloroform (CDH) were used without any further purification. Distilled water was used throughout the course of study.

#### 2.3. Electrospinning set up

The entire equipment consists of the following parts:-

##### 2.3.1 Spinning unit

- Spinning Chamber
- Syringe pump
- Drum / Disc/Plate collector
- Translation stage –for syringe pump
- Translation stage – distance between collector and syringe.
- Shorting stick
- Syringe
- Hamilton Needle
- Stick to remove coagulates from tip

### 2.3.2 Control unit

- a. HV Power supply control
- b. Syringe pump control
- c. Drum collector control
- d. Syringe translation stage control
- e. Plate translation stage control
- f. Distance adjustment control



**Figure 2.1:** Setup of an electrospinning unit (ESPIN-NANO (PHYSICS EQUIPMENT CO.))

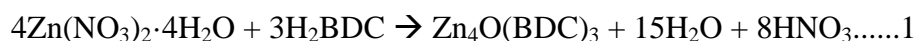
### 2.3.3 Preparation of Polystyrene nanofibers

Polystyrene nanofibers of different concentration and at different flow rates were prepared by electrospinning technique. For this purpose, homogeneous polystyrene solutions were prepared by dissolving different amounts of polystyrene (5-20 % w/v) in DMF/CHCl<sub>3</sub> (1:4) at room temperature.

## 2.4 Preparation of Supramolecular assembly of Metal Organic

### frameworks[Zn<sub>4</sub>O(BDC)<sub>3</sub>, MOF-5]

The procedure to synthesize one of the most celebrated MOF relies on the supramolecular assembly of zinc ions with benzene dicarboxylic acid (BDC) in the presence of a suitable medium, the solvent usually belonging to the subclass of formamides. The formal equation for the reaction involved in the formation of MOF-5 is presented in equation 1



MOF-5 was prepared by the self-assembly of zinc nitrate with terephthalic acid. In brief, a separate solution of BDC (5.06 g, 30.5 mmol) and zinc acetate dihydrate (16.99 g, 77.4 mmol) was prepared in DMF, which were mixed and allowed to react for 2.5 h under stirring. The resulting crystallites were filtered, washed repeatedly with DMF and stored in a desiccator.

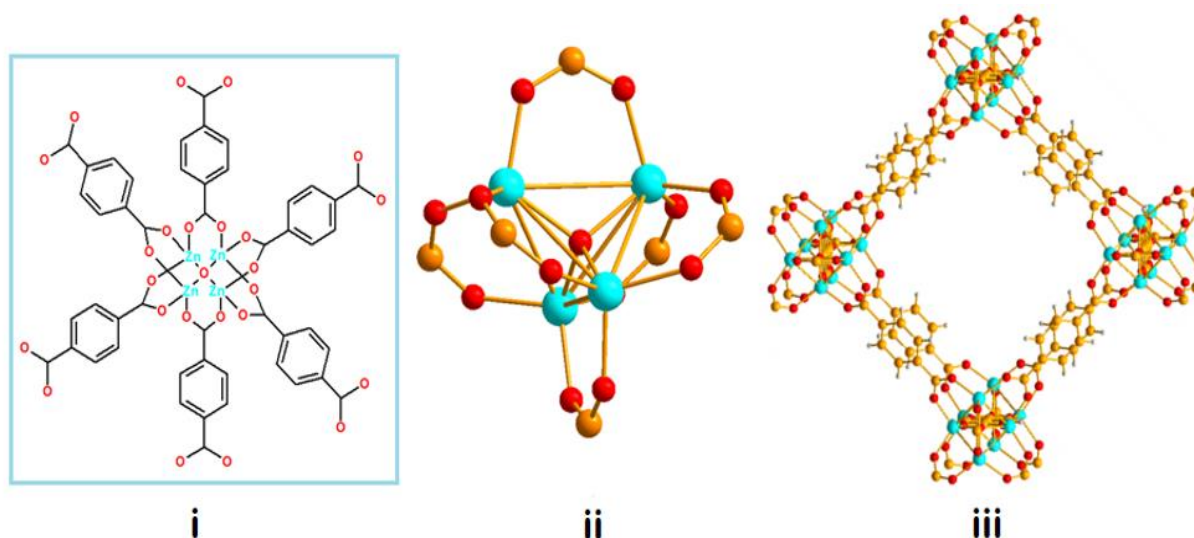


**Figure 2.2:** Chemical structure of secondary building unit, ii) structure of Zn<sub>4</sub>O node and iii) 3 D structure of the framework of MOF-5 (Zn: cyan; C:grey; H:White and O:red)

## 2.5 Ultrasonication

Ultrasonic processor Sonics vibra-cell VCX 500 (500 watts) was used for the uniform distribution and dispersion of MOF-5 in polystyrene solution. The amplitude was set at 40%

with pulse rate of 15 seconds and timer was set for 30 minutes. The beaker used was kept in ice bath throughout the process. A picture of the instrument used is presented in Figure 2.3.



**Figure2.3:** Ultrasonicator used for dispersion of MOF-5 in polystyrene solution

## **2.6 Preparation of MOF5 immobilised polystyrene nanofibers**

For the purpose of preparation of MOF-5 immobilised polystyrene nanofibers, different amount of MOF-5 (20-500 % w/w PS) was dispersed in polystyrene solution. The concentration of polystyrene solution was maintained at 15% (w/v). The solution was ultrasonicated for 2 h. A hypodermic syringe (5ml capacity) was fitted with Hamilton needle(inner diameter 1.3 mm, .15 mm thickness outer diameter 1.6 mm)and filled with the polymer solution containing MOF-5. The syringe was placed horizontally onto the syringe holder. The flow rate was set in the pump and a potential gradient was applied across the needle and the collector. A plate collector was used for collecting the unaligned or random fibers. The collector was enveloped with aluminum foil on the side facing the needle for the ease of taking out the formed nanofibers from the plate. Once this set up was completed, the

electrospinning assembly was closed and the flow rate was varied (1-2 ml/h). The distance between the needle and collector was maintained at 17 cm. A potential of 20kV was applied between the two ends. The polymer droplets, spherical in shape transformed themselves into a cone shaped that eventually resulted in the generation of a charged jet of a polymer solution, which in turn formed fibers travelling all the way to the collector. The polymer jet experienced bending and whipping instabilities and the jet path was chaotic. The randomly oriented non-woven nanofibrous mat obtained on the collector was removed with utmost care by turning the voltage to zero and complete switching off the setup followed by the use of a discharging stick to ground any residual charge that remained on the needles. Care was taken not to use bare hands prior to discharging and not to disturb the machine while operating. The sample designations are presented below

**Table 2.1:** Sample designation

Sample designation	Amount (g)	
	PS	MOF -5
MOF2PS	100	20
MOF4PS	100	40
MOF6PS	100	60
MOF8PS	100	80
MOF10PS	100	100
MOF20PS	100	200
MOF30PS	100	300
MOF 40PS	100	400
MOF-50PS	100	500



## **2.7. Characterization**

### **2.7.1 Structural characterization**

#### **2.7.1.1 Scanning Electron Microscopy**

The surface morphology of MOF-5, Polystyrene Nanofibers and MOF-5 immobilised polystyrene nanofibers was studied using a Scanning Electron Microscope (Zeiss EVO MA15) under an acceleration voltage of 20 kV. The morphology of samples was carefully examined which were mounted on aluminium stubs and sputter-coated with gold and palladium (10 nm) using a sputter coater (Quorum-SC7620) operating at 10-12 mA for 120 s.

#### **Principle:**

The scanning electron microscope (SEM) uses a focused beam of high-energy electrons to produce multiple signals generated by electron-sample interactions at the surface of solid specimens. These signals include secondary electrons (that create SEM images), backscattered electrons (BSE), diffracted backscattered electrons (EBSD that are utilised to determine crystal structures and orientations of minerals), photons (characteristic X-rays that are used for elemental analysis), visible light (cathode luminescence--CL), and heat. Secondary electrons and backscattered electrons are used basically for samples imaging: secondary electrons are most vital for showing surface morphology and topography of samples and backscattered electrons are vital for showing contrasts in a composition in a multiphase sample (i.e. for rapid phase discrimination).

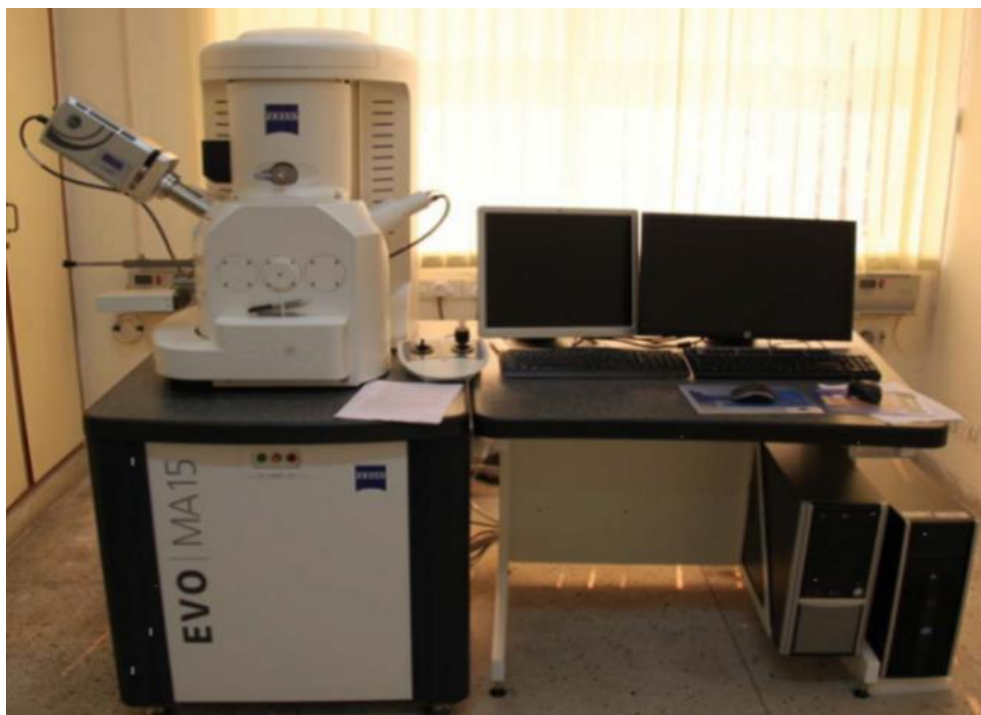


**Figure 2.4:** Scanning electron microscope

### 2.7.1.2 Powder X-rays Diffraction

PXRD data of MOF-5 immobilised polystyrene nanofibers were collected on Bruker D8 advanced diffractometer using Nickel filter Cu-K $\alpha$  radiation. Data were collected with a step size of 0.02° and at count time of 1 sec per step over the range of 5°- 50° (2 $\theta$  value) for the solid.

**Principle:** X-ray powder diffraction (XRD) is a fast analytical technique chiefly used for phase determination of a crystalline material and can also be used to get information about unit cell dimensions. The analyzed material is finely ground, homogenized, and average bulk composition is calculated. X-ray diffraction is based on constructive interference of monochromatic X-rays with a crystalline sample. These X-rays are produced by a cathode ray tube, which is then filtered to generate monochromatic radiation, collimated to condense, and directed to the sample. The interaction of the incident rays with the sample cause constructive

interference and a diffracted ray is produced, when conditions satisfy Bragg's Law ( $n\lambda=2d \sin \theta$ ).

### 2.7.2 FTIR

Fourier Transform Infrared (FT-IR) spectra of MOF-5 and MOF-5 immobilised polystyrene nanofibers were recorded using a Thermo scientific FT-IR (NICOLET 8700) analyzer with an attenuated total reflectance (ATR) crystal accessory. The angle of incidence of the germanium ATR crystal used was characteristically  $45^\circ$  and the spectra was recorded in the wavelength range  $4000\text{-}500 \text{ cm}^{-1}$ , with a resolution of  $4 \text{ cm}^{-1}$ .



**Figure 2.5:** FTIR

**Principle:** FTIR reckons on the fact that most of the molecules absorb light in the infra-red range of the electromagnetic spectrum. This absorption corresponds particularly to the bonds of the molecule. The frequency range is calculated as wave numbers over the range of  $4000 - 600 \text{ cm}^{-1}$ .

The background emission spectrum of the Infra-Red source is recorded, followed by the emission spectrum of the Infra-Red source with the sample in place. The ratio of the sample emission spectrum to the background emission spectrum is directly related to the sample's

absorption spectrum. The resultant absorption spectrum due to the bond natural vibrational frequencies shows the presence of different chemical bonds and functional groups in the sample. FTIR is specifically useful for identification of organic molecular groups and compounds because of functional groups, side chains and cross-links involve will have characteristic vibrational frequencies in the infra-red range.

## 2.7.3 Thermal Characterization

### 2.7.3.1 Thermogravimetric Analysis

The thermal behaviour of MOF-5, polystyrene nanofibers , MOF-5 immobilised polystyrene nanofibers was investigated using Perkin Elmer Diamond STG-DTA under Nitrogen atmosphere (flow rate = 200 ml/min) in the temperature range 50-800 °C. A heating rate of 10 °C/min and sample mass of  $5.0 \pm 0.5$  mg was used for each experiment.



**Figure 2.6:** Thermogravimetric analysis

## Principle

Thermogravimetric analysis (TGA) relies on the measurement of mass loss of material as a function of temperature. In this analytical technique when a material is heated at a uniform rate or kept at a constant temperature a continuous graph of mass change versus temperature is obtained. The measurement is generally carried out in air or in an inert atmosphere and the mass loss is recorded against increasing temperature. A plot of mass change versus temperature ( $T$ ) is considered as the thermo gravimetric curve (TG curve).

### 2.7.3.2. Differential Scanning Calorimetry

The changes in the thermal properties of the MOF-5 immobilised polystyrene nanofibers were investigated using DSC (TA instruments, Q 20 module) under the nitrogen atmosphere. Approximately 4mg of the sample was placed in a 40  $\mu$ L aluminium cap without the pin and sealed with a lid. After erasing the thermal history of samples, they were subjected to a controlled heating programed at 10  $^{\circ}\text{C min}^{-1}$ . Glass transition temperature of the sample was estimated from the graph.



**Figure 2.7:** DSC

**Principle:** Differential scanning calorimetry or DSC is a thermo-analytical technique in which the difference in the amount of heat required to increase the temperature of a sample and a reference are calculated as a function of temperature. Both the sample and reference are kept at the same temperature during the analysis. Mostly the temperature program for a DSC analysis is designed in such a manner that the sample holder temperature increases linearly as a function of time. The reference sample which is to be scanned must have a well-defined heat capacity over the range of temperatures.

The basic principle of this technique is that when the sample goes through a physical transformation such as phase transitions, more or less heat will flow to the sample than the reference in order to maintain both of them at the same temperature. The less or more heat that flows to the sample will depend on whether the transition is exothermic or endothermic in nature.

#### **2.7.4 Surface area analysis**

Surface area investigations were performed using N<sub>2</sub> adsorption-desorption studies on a Surface Area Analyzer (Micrometrics ASAP 2020). For this purpose, the sample was initially degassed under vacuum (10<sup>-6</sup> Torr) at elevated temperature (200 °C) for 16 h following which nitrogen adsorbate was pulsed at 77 K.



**Figure 2.8:** Surface area analyzer

**Principle:** Surface Area Analyzer is used for calculation of surface area. BET surface area is an intrinsic property of powdered porous materials. Surface Area can be calculated using Physical adsorption because physically adsorbed molecules are not bound to specific sites and are free to spread over the entire Surface. Surface Area Analyzer is based on dynamic BET principle. Nitrogen gas is generally used for adsorption. The dynamic flow method uses a highly sensitive thermal conductivity detector to quantify the variation in the concentration of an adsorbate / carrier gas mixture during the process of adsorption or desorption. It measures the surface area at a single point and can be enhanced to measure surface area at multiple points and can also be used to calculate the total pore volume with different gas mixture percentage.

## CHAPTER 3

### RESULTS AND DISCUSSION

#### 3.1 Supramolecular assembly of MOF-5.

The formation of cubic MOF-5 crystals is a result of coordination of Zinc ions with benzene dicarboxylate ligands [21-23]. The morphology of MOF-5 was studied using scanning electron microscopy. Cubic MOF-5 crystals can be seen in the SEM image of MOF-5 as shown below in Figure 3.1.

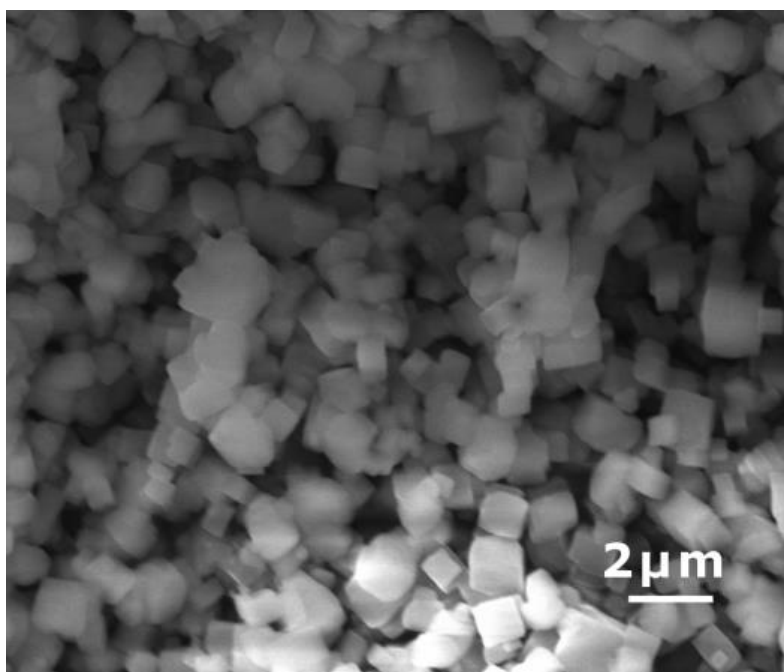


**Figure 3.1:** SEM micrograph of MOF-5

#### 3.2 Surface area analysis of MOF-5

The adsorption-desorption isotherm of nitrogen at 77 K is provided in Figure 3.2. Open and closed circles indicate adsorption and desorption data respectively. The BET surface area was found to be  $620 \text{ m}^2 \text{ g}^{-1}$ . MOF-5 exhibits an average pore diameter of  $18.6 \text{ \AA}$ , which is in the microporous range i.e. diameter pore size is less than  $20 \text{ \AA}$ .



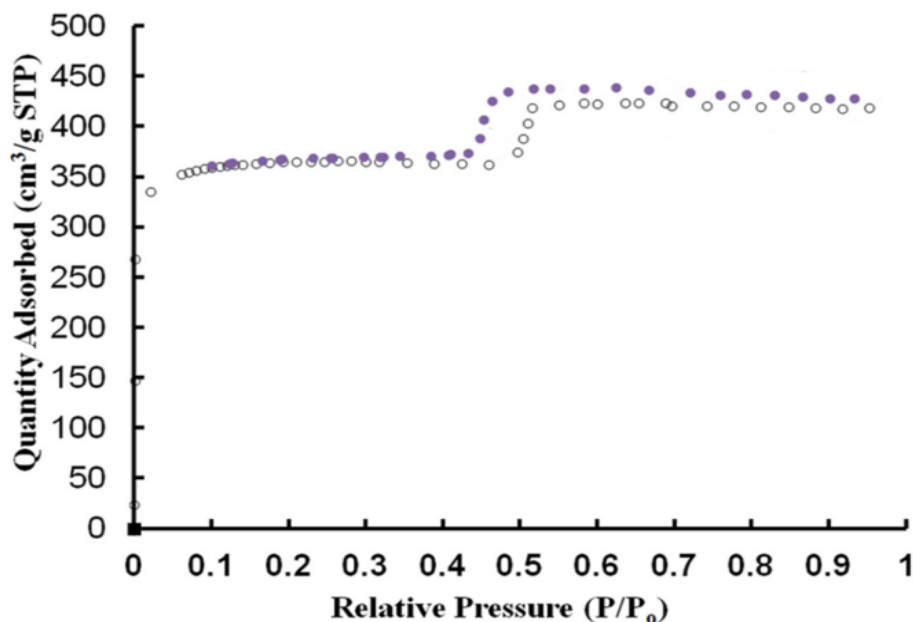


**Figure 3.2:**  $N_2$  adsorption (open circle) and desorption isotherms (closed circle) for MOF5.

### 3.3 Thermal analysis of MOF-5

TG-DTG trace of MOF-5 is shown in Figure 3.3. The initial mass loss of less than 5% up to 300°C can be attributed to the removal of excess DMF which remained entrapped in the framework. This was followed by a pyrolytic decomposition at 410°C leaving a char content of 42% at 600°C.

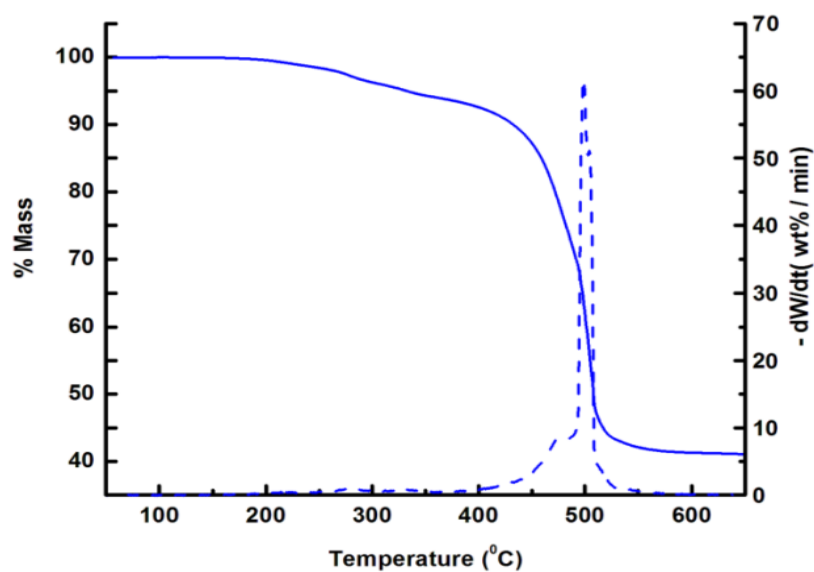


**Figure 3.3:** TG-DTG traces of MOF-5

### **3.4 Electrospinning of polystyrene nanofibre**

Polystyrene solution was electrospun at different concentrations and flow rates to form nanofibers. Scanning electron microscopy was used to study the morphology of the spun fibers.

#### **3.4.1 Effect of Concentration on the polystyrene fibre morphology**

SEM images of electrospun nanofibers prepared using polystyrene at varying concentrations (5-20 % (w/v)) are presented in Figure 3.4 below. It can be seen that at low concentration, beaded morphology is obtained and the beads concentration decreases substantially, with the increase in the concentration of the polystyrene solution. It is visible from the image that the smooth bead less fibers could be obtained at the higher concentration of polystyrene (conc. > 15% w/v) without breaking of a jet during the electrospinning process. This is due to an increase in the polymer chain entanglements caused by an increase in viscosity as a result of higher polymer concentration, which leads to smooth and continuous fibers. It is important to mention that below 5 % (w/v) concentration, fibers are not formed due to fewer chain entanglements in the solution, because of low viscosity and high surface tension of the polystyrene drop. At the concentration of 10% (w/v), fewer small size beaded fibers are obtained. Uniform bead free fibers are obtained at polymer concentrations of 15-20 % (w/v), moreover, the further increment in concentration is impractical because of the very high viscosity of the solution.

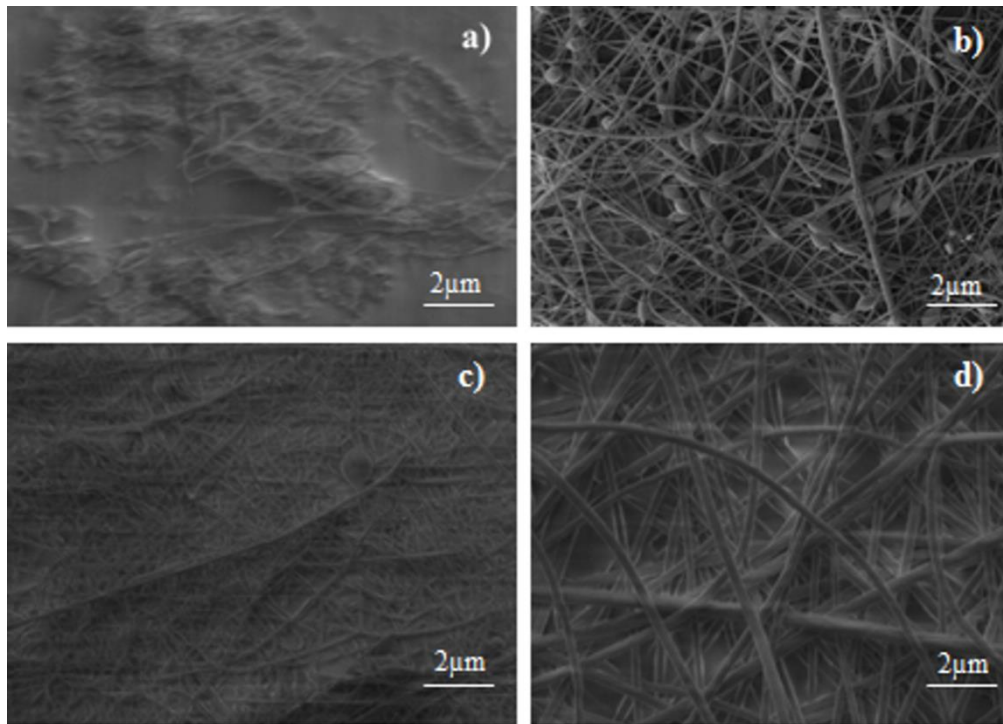


**Figure 3.4:** Effect of concentration on the surface morphology of polystyrene nanofibers at different concentrations: **(a)** 5% (w/v) **(b)** 10% (w/v) **(c)** 15% (w/v) **(d)** 20% (w/v)

### 3.4.2 Effect of flow rate on polystyrene Nanofibre morphology

Flow rate plays a vital role determining the fiber size distribution of the nanofibers. At the flow rate of 1ml/h, the polymer drop emerging from the needle tip has enough time to undergo polarization, which in turn leads to stretching of polystyrene drop and results in fibers formation with significantly small diameter. With the increment in the flow rate from 1ml/h to 2ml/h, the diameter of fiber increases, as interpreted from Figure 3.5.

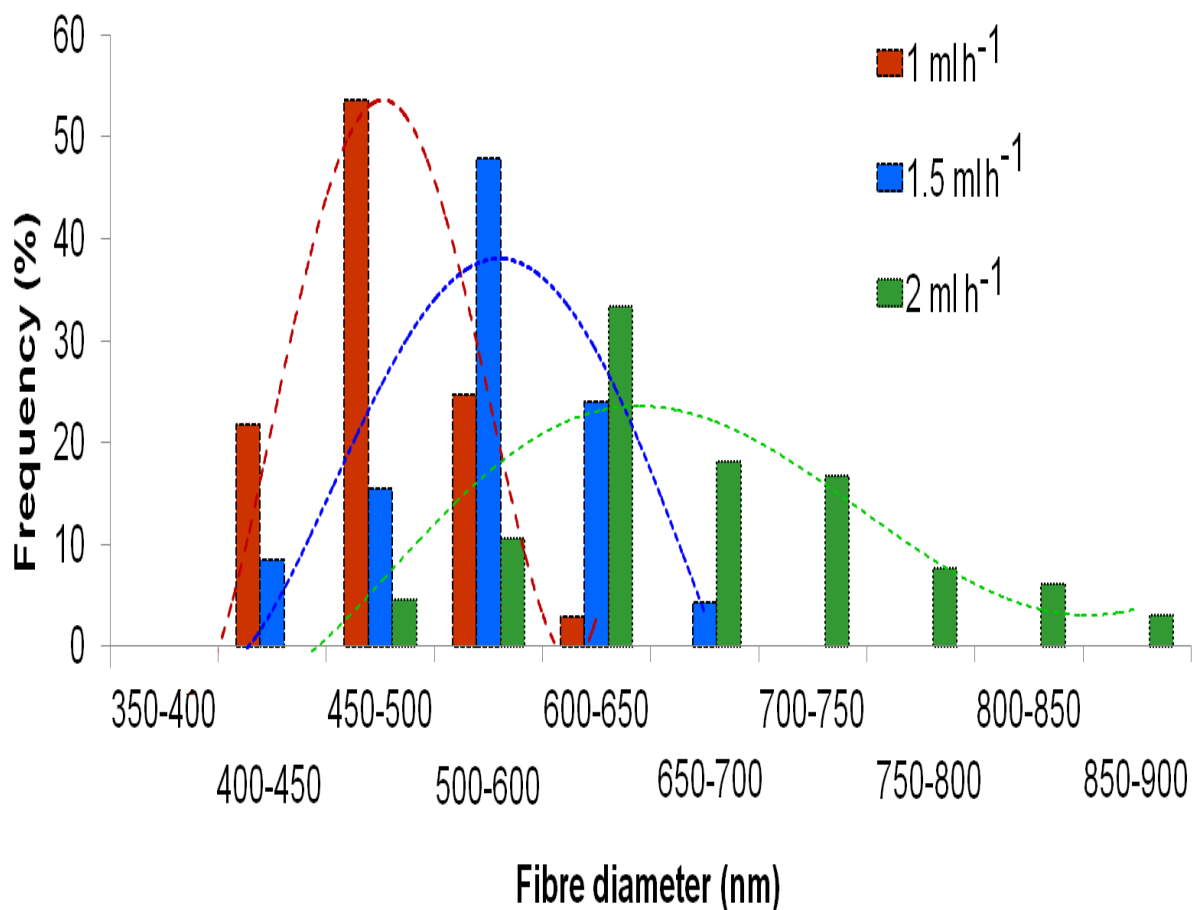


**Figure 3.5:** Effect of flow rate on fiber size distribution of polystyrene at different flow rates

### 3.4.3 Thermal characterization of Polystyrene nanofibers

The Thermo-gravimetric analysis was performed to gain insight about the thermal stability of the samples. The TG-DTG trace of polystyrene fibers is shown in Figure 3.6. TGA trace indicates the residual mass or mass loss as a function of temperature which is shown by the solid line. The DTG trace, a derivative of the mass loss as a function of temperature, is also shown in the figure. The significance of the DTG trace is that even small changes involving a small amount of weight loss can be seen. It can be concluded from the TG traces that polystyrene exhibits a single step degradation with a mass loss of ~98% at 500 °C.

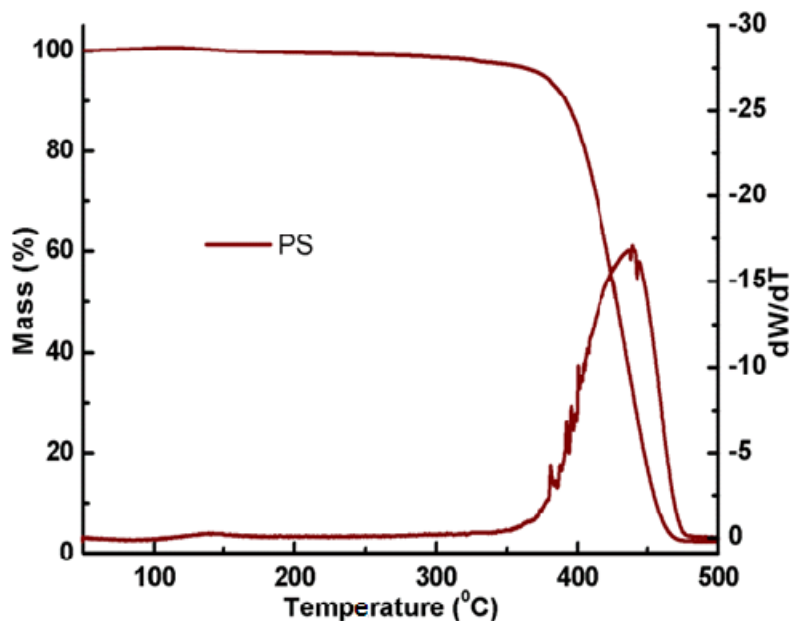


**Figure 3.6:** TG-DTG traces of polystyrene nanofibers

### 3.5. MOF-5immobilised polystyrene fibers

#### 3.5.1 Surface morphology of MOF-5immobilised polystyrene fibers

Varying amounts of MOF-5 (20-500 % w/w PS) was dispersed in polystyrene solution (15% w/v of DMF:CHCl<sub>3</sub>::1:4) in order to obtain MOF-5immobilised polystyrene fibrous mat. The effect of increasing MOF-5 concentration on the polystyrene nanofibers is presented in Figure 3.8. The cubic morphology of the MOF-5 can be observed in the SEM images captured at much higher magnification (Figure 3.7). It can be concluded from the image that higher loadings of MOF can be immobilised in the fibers by increasing the amount of MOF in the solution. Interestingly, very high loadings of MOF-5 (500%) could be achieved, which is hitherto unreported. This can be attributed to the usage of ultrasonication, which causes homogenous distribution and dispersion of MOF-5 in polystyrene solution. In addition, the formation of fibers at such high loadings of MOF-5 is possible due to the usage of Hamilton needle with much higher diameter than conventional syringes. However, as the concentration of MOF-5 was increased further (conc.>500% w/w), nanofibers could not be electrospun.

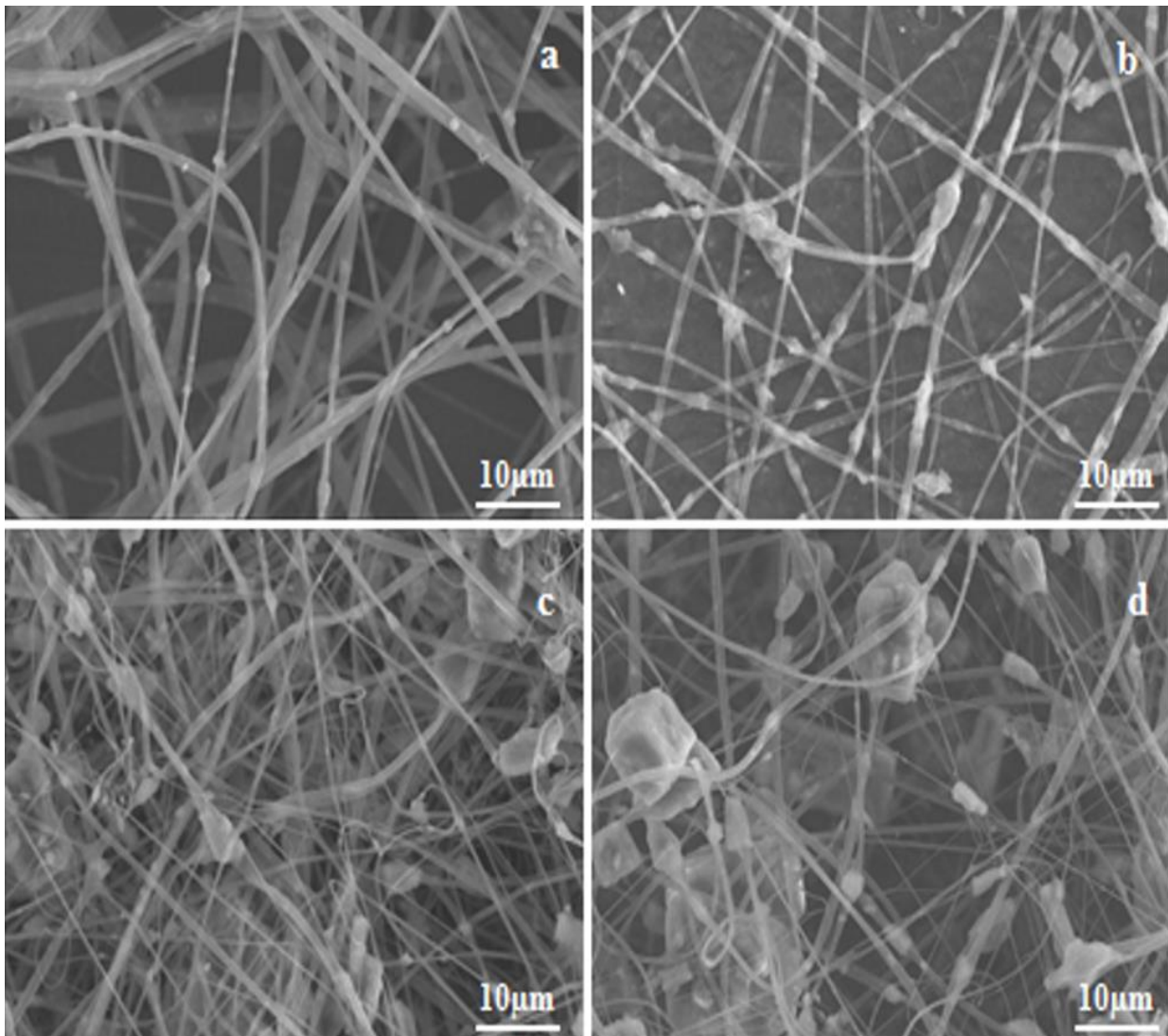


**Figure 3.7:** SEM micrographs of MOF-5 immobilised polystyrene fibers at a flow rate of 1.5 ml/h with MOF-5 concentration of a) 20% b) 100% c) 300% and d) 500%

In a previous study, maximal loading of the composite with MOF of about 40 % could be achieved [1]. The same was attributed to the difference in the polarity of the polymer and the framework. Interestingly in our present study, we were able to load as high as 84% MOF-5 while retaining the fiber-like morphology. This can be attributed to the homogenization of MOF-5 using ultrasonication and use of a larger needle.

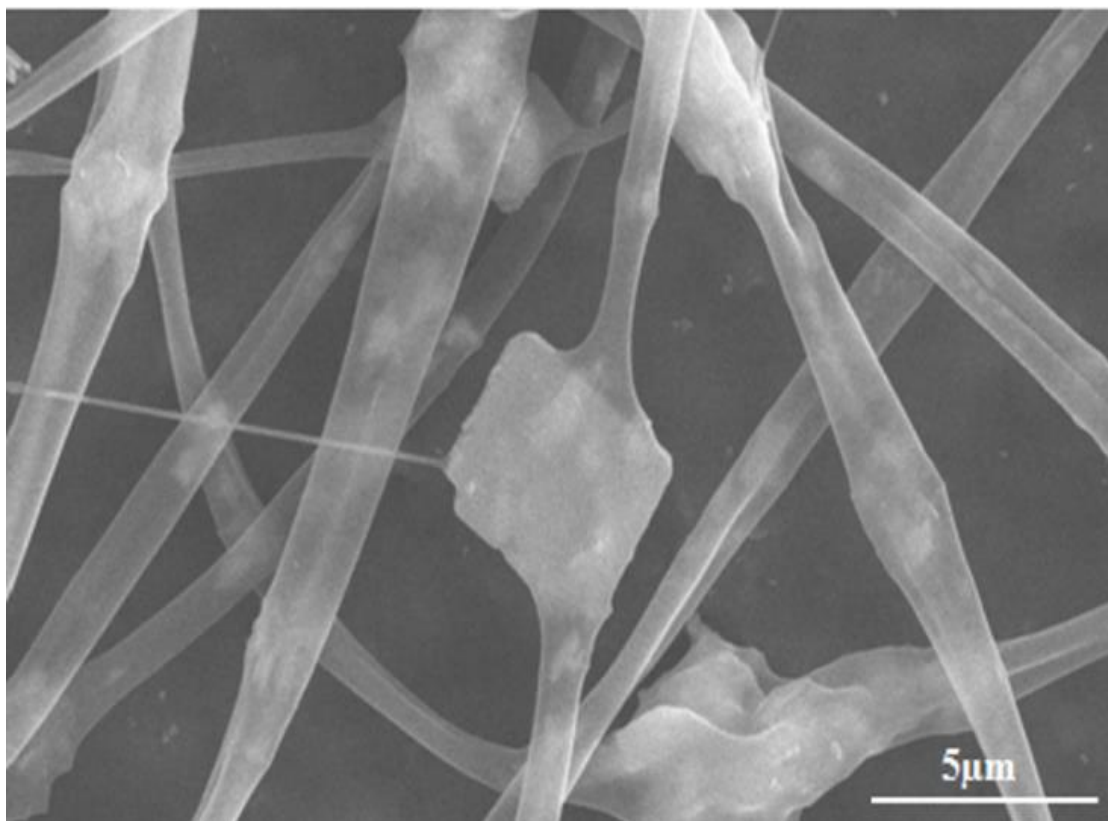


**Figure 3.8:** SEM micrograph of MOF-5 crystal on polystyrene fiber

### **3.5.2 Thermal analysis of MOF-5 immobilised polystyrene fibers**

#### **3.5.2.1. Thermo gravimetric analysis of MOF-5 immobilised polystyrene fibers.**

The TG traces of MOF-5immobilised PS fibers are presented in Figure 3.9. As expected, increasing the amount of MOF-5 led to larger char content. Characteristic decomposition parameters like  $T_{\text{onset}}$ ,  $T_{\text{max}}$  and  $T_{\text{end}}$  are presented in Table 3.1. Polystyrene reportedly undergoes pyrolytic decomposition via chain unzipping reaction at 375 °C. The char content primarily results from the decomposition of zinc terephthalate into zinc oxide. Theoretically

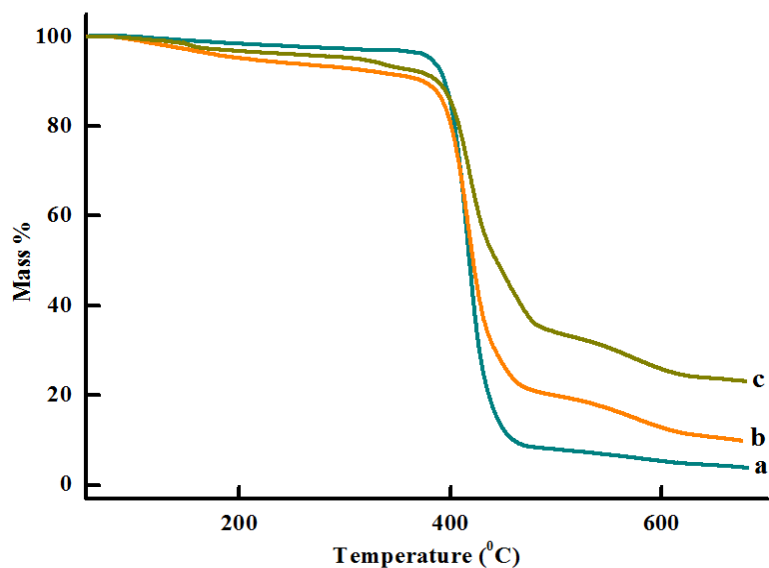


**Figure 3.9:** TG traces of a) MOF2PS b) MOF8PS c) MOF20PS

**Table 3.1** Thermal Characteristic of decomposition

Sample	T <sub>onset</sub> (°C)	T <sub>max</sub> (°C)	T <sub>end</sub> (°C)	Chat content at 600°C (Mass %)
MOF2PS	399.73	418.11	433.62	5.28
MOF8PS	399.33	416.17	436.86	12.73
MOF20PS	398.69	417.43	446.94	25.9

### 3.5.2.2 Differential Scanning Calorimetry of MOF-5 immobilised polystyrene fibers.

DSC traces shown in Figure 3.10 provides the glass transition temperature of polystyrene, which came out to be 95° C as reported earlier. The curve also confirms that MOF-5 do not undergo phase transition in the temperature range in which the characterisation is performed which was expected.



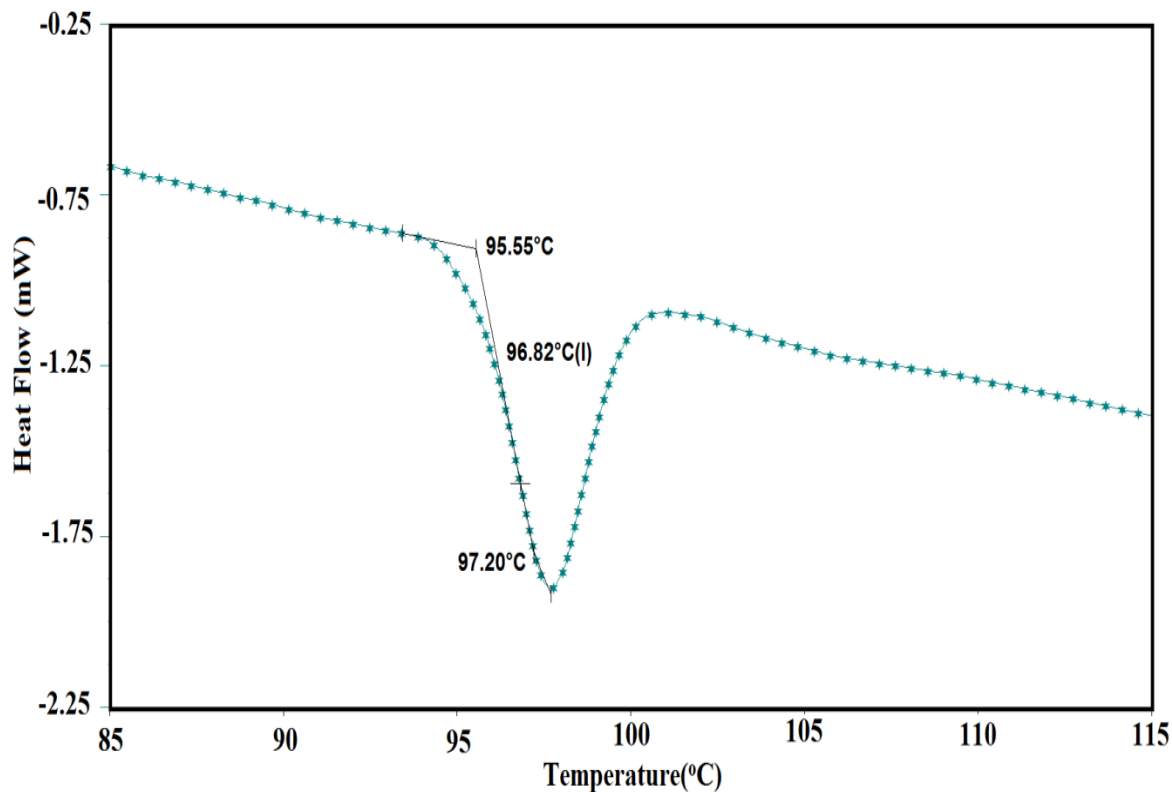


**Figure 3.10:** DSC traces of MOF-5 loaded PS fibers.

### 3.5.4 Crystal structure of MOF-5 immobilised polystyrene fibers.

The structural integrity of the MOF-5 was examined using powder XRD. The PXRD pattern of MOF-5 immobilised Polystyrene fibers is presented in Figure 3.11. It can be seen that the PXRD of MOF-5 exhibit distinct diffraction peaks, characteristic of the crystalline nature of MOF. The peak positions match with the powder pattern generated by Crystallographic Information File (CCDC-277428).

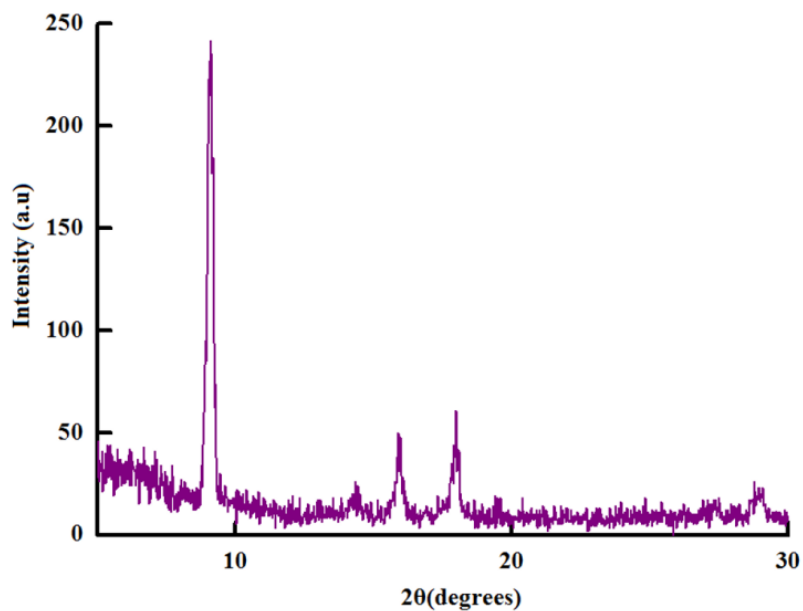


**Figure 3.11:**The PXRD of MOF-5 loaded PS(MOF40PS)

### 3.5.5 FTIR of MOF-5 immobilised polystyrene fibers.

The presence of MOF-5 in the fibers is further corroborated by FT-IR analysis, which was conducted on selected samples and presented in Figure 3.12.

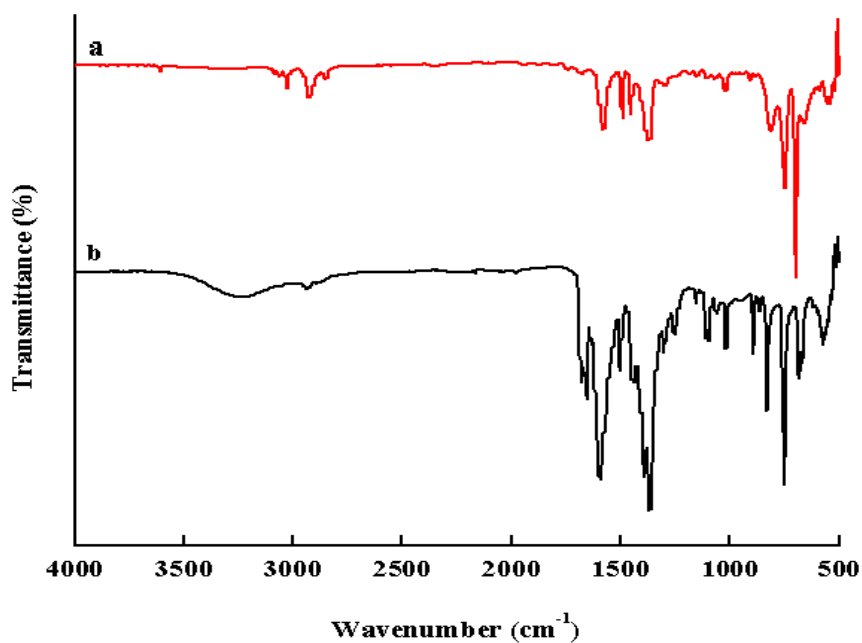


**Figure 3.12:** FTIR spectra of a) PS8MOF b) MOF-5

Characteristic peaks associated with C-H aliphatic and aromatic vibrations were observed in the FTIR spectra of MOF immobilised polystyrene fibers at 2922 and 3026  $\text{cm}^{-1}$  respectively. The structural changes occurring as the ligands and metal ions assemble to form a MOF was also followed by FTIR spectroscopy. The spectra of the terephthalic acid and MOF -5 are also presented in Figure 3.13 for ready reference. Two different CO absorption bands at 1676  $\text{cm}^{-1}$  and 1281 $\text{cm}^{-1}$  were observed in the spectra of TPA which could be attributed to the presence of different types of CO bonds. Due to the coordination of the carboxylic acid groups with the metal ions, a significant shift in the position of the CO absorption band, from 1676  $\text{cm}^{-1}$ , in TPA, to 1657  $\text{cm}^{-1}$  in MOF-5 was observed. Coordination of the linker with the metal ions also led to the disappearance of CO absorption band at 1281  $\text{cm}^{-1}$  and the broad absorption due to the hydroxyl groups  $\sim 3000\text{-}3200 \text{ cm}^{-1}$ . The appearance of peak at 1650  $\text{cm}^{-1}$  indicates a characteristic shift in the peak location for the carboxylate group which occurs due to interaction with the  $\text{Zn}_4\text{O}$  tetrahedra, showing the presence of bonding between organic and metal species. The peak present at 1435  $\text{cm}^{-1}$  indicates deprotonated carboxylic acid bonded to the MOF-5 metal centre suggesting bonding indicative of MOF-5.

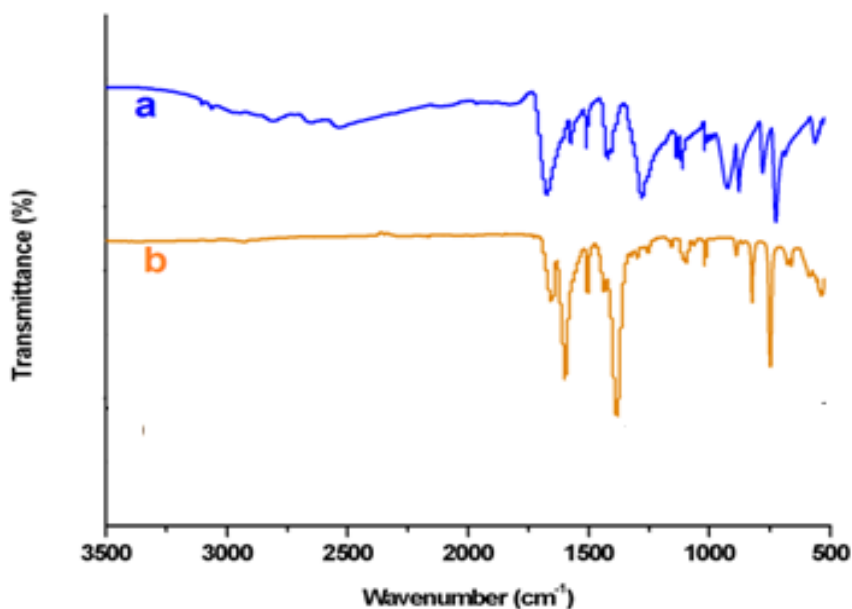


**Figure 3.13:** FTIR spectra of a) TPA b) MOF-5

## CHAPTER 4:

### SUMMARY AND CONCLUSION

The present work deals with the immobilisation of a representative Metal organic framework (MOF-5) in polystyrene nanofibers, with an aim to prepare air filtration membranes for adsorption of toxic gases. For this purpose polystyrene fibers containing different MOF loadings were prepared by electrospinning process. For preparation of nanofibers, the following operating parameters were optimised.

**Concentration :** With increase in the concentration of polystyrene, the morphology of the electrospun fibers shifted from a beaded to smooth continuous fibers. Perfect fibers could be obtained at concentrations higher than 15% w/v. A  $\text{CHCl}_3$ :DMF solution was chosen as a medium for dissolving polystyrene, the ratio of  $\text{CHCl}_3$ :DMF was kept as 4:1.

**Flow rate:** The effect of flow rate on the fiber size distribution was established. As expected, with increasing flow rates, the fiber size distribution shifted towards higher dimensions.

**Potential difference.** Smooth continuous nanofibers could be electrospun at 20 kV.

MOF 5 immobilised polystyrene nanofibers were prepared while varying the flow rates (1-2 ml/h) while maintaining the polystyrene concentration at 15% w/v in a solution of  $\text{CHCl}_3$ :DMF::4:1.

Ultrasonication was used to homogeneously disperse the MOF within the polystyrene solution. Interestingly, very high loadings of MOF-5 could be achieved, with smooth fibers obtainable even at 84% w/w. However, fibers could not be electrospun with increasing the concentration further. In view of the particle size distribution of as prepared MOF 5, a Hamilton syringe (inner dia 1.3 mm) was found to be suitable for smooth ejection of the MOF-PS dispersion.

The developed method appears to be a viable process for production of textiles possessing adsorptive properties, particularly protective clothing for individual protection against toxic gases e.g. volatile organic compounds. In addition, applications as flexible filter material can also be envisaged, with non-woven mat in macro scale (~cm). Thus, the MOF loaded composite fibers can be regarded as a "MOF textile", which combines the flexibility characteristic of polymeric fibers as well as high adsorptive properties of MOFs.

## REFERENCES

- [1] Rose M, Böhringer B, Jolly M, Fischer R, Kaskel S. MOF Processing by Electrospinning for Functional Textiles. *Advanced Engineering Materials*. 2011;13:356-60.
- [2] Mueller U, Schubert M, Teich F, Puetter H, Schierle-Arndt K, Pastre J. Metal-organic frameworks-prospective industrial applications. *Journal of Materials Chemistry*. 2006;16:626-36.
- [3] Ma S, Zhou H-C. Gas storage in porous metal-organic frameworks for clean energy applications. *Chem Commun*. 2010;46:44-53.
- [4] Liu Y, Wang ZU, Zhou H-C. Recent advances in carbon dioxide capture with metal-organic frameworks. *Greenhouse Gases: Science and Technology*. 2012;2:239-59.
- [5] Sathre R, Masanet E. Prospective life-cycle modeling of a carbon capture and storage system using metal-organic frameworks for CO<sub>2</sub> capture. *RSC Advances*. 2013;3:4964-75.
- [6] Savonnet M, Aguado S, Ravon U, Bazer-Bachi D, Lecocq V, Bats N, et al. Solvent free base catalysis and transesterification over basic functionalised Metal-Organic Frameworks. *Green Chemistry*. 2009;11:1729-32.
- [7] Opanasenko M, Dhakshinamoorthy A, Hwang YK, Chang J-S, Garcia H, Čejka J. Superior Performance of Metal-Organic Frameworks over Zeolites as Solid Acid Catalysts in the Prins Reaction: Green Synthesis of Nopol. *ChemSusChem*. 2013;6:865-71.
- [8] Rowsell JLC, Yaghi OM. Metal-organic frameworks: a new class of porous materials. *Microporous and Mesoporous Materials*. 2004;73:3-14.
- [9] Yilmaz B, Trukhan N, Müller U. Industrial Outlook on Zeolites and Metal Organic Frameworks. *Chin J Catal*. 2012;33:3-10.
- [10] Batten SR, Champness NR, Chen X-M, Garcia-Martinez J, Kitagawa S, Ohrstrom L, et al. Coordination polymers, metal-organic frameworks and the need for terminology guidelines. *CrystEngComm*. 2012;14:3001-4.
- [11] Huang Z-M, -Z ZY, M. K, S. R. A review on polymer nanofibers by electrospinning and their applications in nanocomposites. *Composites Science and Technology*. 2003;63:2223-53.
- [12] Frenot A, Chronakis IS. Polymer nanofibers assembled by electrospinning. *Current Opinion in Colloid and Interface Science*. 2003;8:64-75.
- [13] He M, Xue J, Geng H, Gu H, Chen D, Shi R, et al. Fibrous guided tissue regeneration membrane loaded with anti-inflammatory agent prepared by coaxial electrospinning for the purpose of controlled release. *Applied Surface Science*. 2015;335:121-9.
- [14] Pham QP, Upma Sharma, Mikos AG. Electrospinning of Polymeric Nanofibers for Tissue Engineering Applications: A Review. *Tissue Engineering*. 2006;12.
- [15] Abdelgawad AM, Hudson SM, Rojas OJ. Antimicrobial wound dressing nanofiber mats from multicomponent (chitosan/silver-NPs/polyvinyl alcohol) systems. *Carbohydrate Polymers*. 2014;100:166-78.
- [16] Li Y, Huang Z, Lü Y. Electrospinning of nylon-6,6,1010 terpolymer. *European Polymer Journal*. 2006;42:1696-704.
- [17] Yang E, Qin X, Wang S. Electrospun crosslinked polyvinyl alcohol membrane. *Materials Letters*. 2008;62:3555-7.
- [18] Khatri Z, Ali S, Khatri I, Mayakrishnan G, Kim SH, Kim I-S. UV-responsive polyvinyl alcohol nanofibers prepared by electrospinning. *Applied Surface Science*. 2015;342:64-8.
- [19] Fashandi H, Karimi M. Pore formation in polystyrene fiber by superimposing temperature and relative humidity of electrospinning atmosphere. *Polymer*. 2012;53:5832-49.
- [20] Avinash B, Mai Y-W, Wong S-C, Abtahi M, Chen P. Electrospinning of polymer nanofibers: Effects on oriented morphology, structures and tensile properties. *Composites Science and Technology* 2010;70:703-18.
- [21] Manju, Kumar Roy P, Ramanan A, Rajagopal C. Post consumer PET waste as potential feedstock for metal organic frameworks. *Materials Letters*. 2013;106:390-2.
- [22] Manju, Roy PK, Ramanan A. Toughening of epoxy resin using Zn<sub>4</sub>O (1,4-benzenedicarboxylate)<sub>3</sub> metal-organic frameworks. *RSC Advances*. 2014;4:52338-45.
- [23] Manju, Roy PK, Ramanan A, Rajagopal C. Core-shell polysiloxane-MOF 5 microspheres as a stationary phase for gas-solid chromatographic separation. *RSC Advances*. 2014;4:17429-33.